J. Chem. Thermodynamics 125 (2018) 189–199

Contents lists available at ScienceDirect

J. Chem. Thermodynamics

journal homepage: www.elsevier.com/locate/jct

Solubilities in aqueous solutions of the sodium salts of succinic and glutaric acid with and without ammonium sulfate

Keith D. Beyer *, Lukas G. Buttke

Department of Chemistry & Biochemistry, University of Wisconsin-La Crosse, La Crosse, WI 54601, USA

ARTICLE INFO

Article history:
Received 26 February 2018
Received in revised form 31 May 2018
Accepted 2 June 2018
Available online 4 June 2018

Keywords:
Ammonium sulphate
Sodium malonate
Sodium succinate
Aqueous
Phase diagram
Solubility

ABSTRACT

The aqueous solubility of the least soluble salts in mixtures of sodium hydrogen succinate, sodium succinate, sodium hydrogen glutarate, and sodium glutarate with and without ammonium sulfate present has been studied. Solubility temperatures were determined in solutions of known concentration using Differential Scanning Calorimetry. The identity of the least soluble solid was determined by a combination of X-ray crystallography and infrared spectroscopy. The identified solids included ammonium sulfate, sodium sulfate, sodium ammonium sulfate dihydrate (lecontite), sodium hydrogen succinate, sodium succinate hexahydrate, sodium hydrogen glutarate dihydrate, and ammonium hydrogen glutarate. Of the 16 series of solutions studied, lecontite was most frequently the least soluble solid.

1. Introduction

Field measurements have shown that the major chemical components of aerosols in the free and upper troposphere (UT) include organic and inorganic compounds and mineral dust [1,2], with the most abundant inorganic components being ammonium and sulfate [3]. With respect to the organic fraction, dicarboxylic acids (DCA) have been found in a range of environments, particularly for aerosols that have undergone chemical aging [4]. Both primary organic and secondary organic aerosols have been found to contain DCA [3], and their concentration in aerosols is increasing [5]. Field measurements have shown that succinic and glutaric acids are among the most abundant DCA in atmospheric aerosols [5–7]. Mineral dust has also been observed in aerosols, especially under acidic conditions, where mineral dust components can be reacted to the aqueous phase through chemical aging [8,9] The aqueous phase chemistry of aerosols can be enhanced by metals at the surface or reacted into the aerosol interior [8,10]. The presence of organics, metals, and metal salts have been shown to be present in large numbers of aerosols in field studies with sources of sea spray (Na, Mg) [4,11–13], biomass burning (K) [14,15], and mineral dusts and meteoritic material (Na, K, Ca, Fe) [1,16–19]. Metal ions can displace hydrogen ions from organic acids to form carboxylate salts in atmospheric aerosols as shown by field and lab studies [11,13,20,21]. As an example, a particle that experienced UT temperatures or dry conditions and contained dissolved NaCl and succinic acid could undergo the following:

$$n\mathrm{NaCl}(aq) + \mathrm{H_2C_4H_4O_4}(aq) \rightarrow \mathrm{Na_nH_{2-n}C_4H_4O_4}(s) + n\mathrm{HCl}(aq,g) \quad (1)$$

where n equals one or two (corresponding to the number of acidic hydrogens present in the acid). According to recent studies the HCl product is highly volatile, and the organic salt will remain in the particle since it has a much lower vapor pressure [13,20]. The sodium oxalate salt could precipitate when the particle experiences either cold or dry conditions in the atmosphere [21]. While the solubilities of $NaHC_4H_4O_4$ and $Na_2C_4H_4O_4$ in water are well known [22], the impact of ammonium sulfate on solubility in solutions of the sodium succinates has not been investigated. The solubility of $NaHC_5H_6O_4$ in water has not been previously investigated to our knowledge, and that of $Na_2C_5H_6O_4$ has only recently been investigated [23]. In both cases the effect of ammonium sulfate on solubility in water has not been investigated. In particular, salts other than the sodium oxalates and ammonium sulfate could form from these complex solutions of ions as has been found for similar systems in our lab [24,25].

2. Materials and methods

2.1. Sample preparation

Solutions studied in our experiments were made by mixing chemicals as listed in Table 1 with deionized water. All samples

* Corresponding author.
E-mail address: kbeyer@uwlax.edu (K.D. Beyer).

https://doi.org/10.1016/j.jct.2018.06.002
0021-9614/

were made such that NaOH was in very slight excess. For $NaHC_4H_4O_4$ and $Na_2C_4H_4O_4$ samples, 1.005 ± 0.004 and 2.004 ± 0.007 $NaOH/H_2C_4H_4O_4$ mole ratio solutions were made, respectively. For $NaHC_5H_6O_4$ and $Na_2C_5H_6O_4$ samples, 1.001 ± 0.001 and 2.002 ± 0.003 $NaOH/H_2C_5H_6O_4$ mole ratio solutions were made, respectively. (Throughout this paper values reported as a ± b are mean values (a) with calculated standard deviation (b) = $\sqrt{\frac{\sum^{(x-\bar{x})^2}}{(n-1)}}$, where x is an individual datum, $\bar{x}$ is the mean value, and n is the number of samples).

Infrared spectroscopy was used to identify when ice formed and melted in our samples. The identity of the salt that precipitates from our sample solutions was confirmed by a combination of X-ray crystallography and infrared spectroscopy. Crystal structures were determined at the Molecular Structure Laboratory in the Chemistry Department at the University of Wisconsin-Madison. Details of how these experiments are performed can be found in the Supporting Information of Kissinger et al. [24], which is available free of charge via the Internet at http://pubs.acs.org. Briefly, a single crystal is removed from a saturated solution at room temperature and placed in the instrument for analysis. The identity of the solid is determined by a match of the crystallographic data in the Cambridge Crystallographic Database (CSD) or the Inorganic Crystal Structure Database (ICSD). The identity of the following salts was determined with these experiments: $NaHC_4H_4O_4$ [26], $Na_2C_4H_4O_4{\cdot}6H_2O$ [27], $NaHC_5H_6O_4{\cdot}2H_2O$ [28], $NH_4HC_5H_6O_4$ [29], $NaNH_4SO_4{\cdot}2H_2O$ (lecontite) [30], $(NH_4)_2SO_4$ [31], Na_2SO_4 [32]. Once the identity of these solids was determined for one concentration in a series of experiments with constant concentration of ammonium sulfate, we concluded the pattern of absorption bands in the corresponding infrared spectra constituted the infrared "fingerprint" of that compound. The presence of the unique set of bands in other samples in the concentration series confirmed the presence of the same solid. In addition, consistency (non-discontinuity) in the liquidus temperatures in the concentration series was additional evidence for the presence of the same solid as that identified in X-ray crystallography and infrared spectroscopy experiments.

2.2. Differential scanning calorimetry

Thermal data were obtained with a Mettler Toledo DSC1 instrument. The instrument was purged with high purity nitrogen gas. Our accuracy is estimated to be ±0.9 K with a probability of 0.94 based on a four point temperature calibration using indium, HPLC grade water, anhydrous, high purity (99%+) octane, and anhydrous, high purity heptane (99%+) from Aldrich, the latter three stored under nitrogen. The details of standard temperature calibration and instrument reproducibility can be found in Schubnell [33].

Samples sizes were typically (20 ± 5) mg using 40 μL aluminium pans with sealed lids. A typical experiment consisted of initially cooling the sample from 298 k to 183 K at 10 K per minute. The sample was then held at 183 K for five minutes, and then temperature increased 1 K per minute to 298 K or a temperature that was expected to be at least five degrees above the last phase transition.

2.3. Infrared spectroscopy

Infrared spectra were acquired using a temperature controlled, air sealed cell. Temperature control was achieved by resistive heating from an Omega temperature controller with the cooling source being liquid nitrogen in contact with the cell. Two μL of the liquid sample was placed on a ZnSe window and compressed with a second ZnSe window. These windows were then placed in the cell and held in the IR beam path. Moisture was kept from the sample and windows by placing glass purge tubes on either side of the IR cell and sealed to the cell with Teflon coated o-rings. KBr windows were used on the open ends of these tubes to create an air-sealed environment. The tubes were then purged with dry nitrogen gas. Temperature calibration of the cell was achieved by observing the melting phase transition of several substances: HPLC grade water, decane, octane and acetic anhydride all supplied by Aldrich, and covering the range 273–200 K [34].

A Bruker Tensor 37 FTIR with a DTGS detector at 4 cm^{-1} resolution was utilized for data acquisition. In a typical experiment, samples were cooled from room temperature to a point where it was observed all liquid had crystallized. In cases where all liquid did not crystallize, the lowest temperature of any experiment was approximately 185 K, due to limitations of the sample cell. Warming of the samples to observe melting transitions occurred at approximately 1 K per minute.

3. Results

3.1. Binary systems

3.1.1. $NaHC_4H_4O_4/H_2O$

The solubility of $NaHC_4H_4O_4$ in water has been known for some time and values appear in standard compilations [22,35], though these are based on the work of Marshall and Bain [36]. Two crystals

Table 1
Chemical samples used in this study.

Chemical name	Chemical Formula	Source	Mass fraction purity	Purification Method
Succinic Acid	$C_4H_6O_4$	Sigma-Aldrich	>0.99[a]	None
Glutaric Acid	$C_5H_8O_4$	Acros Organics	>0.99[a]	None
Ammonium Sulfate	$(NH_4)_2SO_4$	Fisher Scientific	>0.99[a]	None
Sodium Hydroxide	NaOH	Fisher Scientific	0.995 ± 0.008[b]	None
Sodium Hydrogen Succinate	$NaHC_4H_4O_4$	*in situ*[c]	[d]	None
Sodium Succinate Hexahydrate	$Na_2C_4H_4O_4{\cdot}6H_2O$	*in situ*[c]	[d]	None
Sodium Hydrogen Glutarate Dihydrate	$NaHC_5H_6O_4{\cdot}2H_2O$	*in situ*[c]	[d]	None
Ammonium Hydrogen Glutarate	$NH_4HC_5H_6O_4$	*in situ*[c]	[d]	None
Sodium Ammonium Sulfate Dihydrate	$NaNH_4SO_4{\cdot}2H_2O$	*in situ*[c]	[d]	None
Sodium Sulfate	Na_2SO_4	*in situ*[c]	[d]	None
Water	H_2O	Municipal	≥0.9999995	R.O. + D.I.[e]

[a] As reported by the supplier.
[b] As determined by titration of NaOH samples with potassium hydrogen phthalate.
[c] These compounds were synthesized from mixtures of commercial compounds in deionized water as described in the text.
[d] Crystals of these compounds did not appear to have impurities from X-ray crystallographic analysis.
[e] Water from the municipal source was purified with a Culligan B-Series Reverse Osmosis (R.O.) system and polished with two Culligan mixed-bed deionizers (D.I.) Purity is as reported by Culligan using conductivity measurements.

form from solution dependent on the concentration of the precipitating solution. For solutions with sodium hydrogen succinate concentration $w \leq 0.39$ (where w is defined as mass fraction solute), $NaHC_4H_4O_4{\cdot}3H_2O$ is the stable solid. At concentrations of $w \geq 0.39$ $NaHC_4H_4O_4$, $NaHC_4H_4O_4$ solid forms from solution. Thus, a $NaHC_4H_4O_4$ concentration of $w = 0.39$ at 311.9 K constitutes a peritectic point. The phase diagram for this system is given in Fig. S1 in the Supplementary material along with the selected concentrations we studied for this system to confirm the literature values. The ice melting points in this system had not been previously studied, and these values are shown in Fig. S1 and listed in Table S1 in the Supplementary material. We determined the eutectic concentration to be $w = 0.198$ $NaHC_4H_4O_4$ by a fit to our ice melting points and the solubility values for $NaHC_4H_4O_4{\cdot}3H_2O$ from Linke. The two equations were solved simultaneously to yield the eutectic concentration. The eutectic temperature was determined to be 265.3 ± 0.8 K from an average of our DSC measurements. A glass transition was observed on warming our samples with an average onset temperature of 210 ± 1 K. Since crystallization events were observed upon warming our samples, it was clear that they had only partially crystallized on cooling, which is confirmed by the observation of constant glass transition temperatures.

3.1.2. $Na_2C_4H_4O_4/H_2O$

This system has also been previously studied with the most complete dataset found in the compilation of Linke [22]. Here, we find the data of Taft and Welch [37] for ice melting points, and Marshall and Bain [36] for salt solubilities, where they determined two salts form from aqueous solution. At $Na_2C_4H_4O_4$ concentration $w \leq 0.455$, $Na_2C_4H_4O_4{\cdot}6H_2O$ is the stable solid, while at higher concentrations it is $Na_2C_4H_4O_4$. The solubility data yields the conclusion that a $Na_2C_4H_4O_4$ concentration $w = 0.455$ and a temperature of 330.1 K is a peritectic point. We measured the ice melting and salt dissolution temperatures for several concentrations of $Na_2C_4H_4O_4$ and found good agreement with the literature data as seen in Fig. S2 in the Supplementary material. The eutectic temperature in this system was found to be 264.3 ± 0.5 K from an average of our DSC samples. We fit literature and our experimental ice melting data as well as literature and our experimental $Na_2C_4H_4O_4{\cdot}6H_2O$ solubility data to polynomial equations and solved them simultaneously to determine a eutectic concentration $w = 0.162$ $Na_2C_4H_4O_4$. Our raw data is given in Table S2 and plotted in Fig. S2 in the Supplementary material along with data from Linke and that of Rozaini and Brimblecombe [23]. It is seen that the solubility temperatures of Rozaini and Brimblecombe are generally lower than those from Linke and our DSC results. This is likely the result of how the experiments of Rozaini and Brimblecombe were performed. They determined solubilities by cooling solutions and noting when crystals appeared. However, supercooling is likely to occur in such experiments, thus leading to lower solubility temperatures than observed when saturated solutions are warmed as in our DSC experiments. We also observed a glass transition on warming our samples with an average onset temperature of 204.6 ± 0.8 K. This represents a glass transition for a concentrated liquid in a partially frozen solution.

3.1.3. $NaHC_5H_6O_4/H_2O$

It appears this system has not been previously studied. We were able to make samples that covered a range of concentrations $w =$ 0.05 to 0.40 $NaHC_5H_6O_4$. A single crystal from a solution that was saturated at room temperature was used for X-ray crystallography analysis. The solid was determined to be $NaHC_5H_6O_4{\cdot}2H_2O$ by a match of the crystallographic data in the Cambridge Crystallographic Database (CSD). This solid was reported in the literature as having the formula $(C_5H_{11}O_5Na)_n$ indicating a polymeric configuration [28]. A sample DSC thermogram is given in Fig. S3 in the Supplementary material for a $w = 0.30$ solution, and in Fig. S4 in the Supplementary material we show the infrared spectra of a solution with the same concentration as it is cooled and warmed showing the changes in the infrared absorbances when ice and $NaHC_5H_6O_4{\cdot}2H_2O$ form. The characteristic shifts in the IR spectrum when the salt crystallizes are given in FTable S3 in the Supplementary material. In both experiments we observe that ice crystallizes on cooling, but the salt does not crystallize until the sample is warmed and just before eutectic melting can occur. This pattern occurred in all of our samples and leads to the conclusion that a significant barrier exists to nucleation of $NaHC_5H_6O_4{\cdot}2H_2O$ from solution. The observed transitions in DSC experiments are plotted in Fig. 1 and listed in Table 2. These data were also fit to second order polynomials and solved to determine the eutectic concentration, w = 0.249 $NaHC_5H_6O_4$. The eutectic temperature of 266.2 ± 0.1 K was determined from an average of the eutectic temperatures of samples in DSC experiments. We observed a glass transition in all samples in the warming segment, with an average value of (208.6 ± 1.7) K.

3.1.4. $Na_2C_5H_6O_4/H_2O$

Solubility data for this system have been reported by Rozaini and Brimblecombe [23] and are given in Fig. S5 along with our ice melting data from DSC experiments, with raw DSC values given in Table S4 in the Supplementary material . The samples we studied covered the range of $w = (0.05–0.40)$ $Na_2C_5H_6O_4$, but in our IR and DSC experiments we were unable to crystallize $Na_2C_5H_6O_4$ in any of our samples. In contrast Rozaini and Brimblecombe observed crystallization in their solutions upon cooling with agitation ($w = (0.37–0.57)$ $Na_2C_5H_6O_4$ solutions); however, their samples sizes were greater than 2.00 mL while ours were 0.02 mL. This gives strong evidence that $Na_2C_5H_6O_4$ has a significant barrier to nucleation and the probability of its formation from solution is strongly volume-dependent. We observed a glass transition in our partially crystallized solutions, with an average onset T_g value of (205.0 ± 0.4) K.

3.2. Ternary systems

We explored the effect of ammonium sulfate (AS) on solutions of the sodium salts of succinic and glutaric acid. Solutions were made adding NaOH and the respective acid in a 1:1 or 2:1 ratio to aqueous solutions, which were also $w_{AS} = 0.1000$, 0.2000, 0.3000, or 0.4000. Multiple crystallization and melting/dissolution transitions were observed in these samples in DSC and IR experiments (an example thermogram for each organic salt studied with ammonium sulfate is given in Fig. S6 in the Supplementary material), although generally the typical melting pattern for a ternary system was observed: ternary eutectic melting, phase boundary melting, and melt (dissolution) of the least soluble solid in its primary phase field. However, in many cases additional thermal transitions occurred; some of which could not be identified as to their source. In this study our focus was on the final melting or dissolving solid (solubility) in solution. Crystals from a solution saturated at room temperature at each ammonium sulfate concentration studied with each organic salt were used for X-ray crystallographic analysis. The results of this analysis are given in Table 3 along with the NH_4^+/Na^+ mole ratio of each sample.

3.2.1. $NaHC_4H_4O_4/(NH_4)_2SO_4/H_2O$

Raw DSC data for this system are given in Table S5 in the Supplementary material. We observe that three salts form from these solutions dependent on the NH_4^+/Na^+ mole ratio: $NaHC_4H_4O_4$ (low ratio), $NaNH_4SO_4{\cdot}2H_2O$ (moderate ratio), $(NH_4)_2SO_4$ (high ratio). We have plotted our complete DSC solubility data in Fig. 2. For a 0.1000 w_{AS} (0.61 NH_4^+/Na^+ mole ratio), $NaHC_4H_4O_4$ is the least

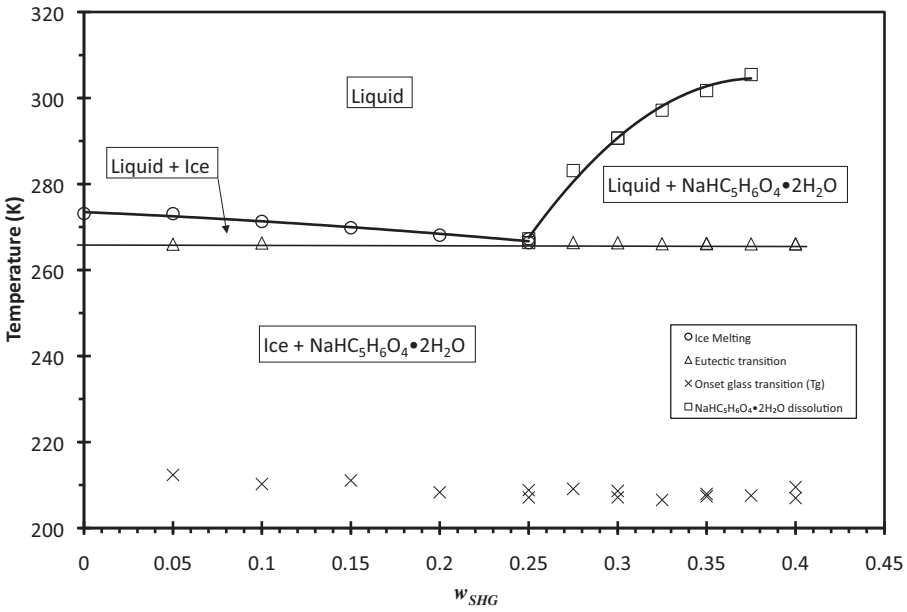

Fig. 1. Partial phase diagram for the $NaHC_5H_6O_4/H_2O$ system constructed from our DSC data, w_{SHG} is the mass fraction $NaHC_5H_6O_4$.

Table 2
DSC data for phase transitions in the $NaHC_5H_6O_4/H_2O$ system, w_{SHG} = mass fraction $NaHC_5H_6O_4$, T_g = glass transition temperature, T_e = eutectic temperature, T_L = liquidus temperature, at pressure 99.2 kPa. [a]

w_{SHG} [b]	T_g/K [c]	T_e/K [c]	T_L/K [c]
Ice primary phase region [d]			
0.0500	212.4	266.0	273.1
0.1000	210.2	266.3	271.3
0.1500	211.1		269.8
0.2000	208.3		268.1
$(NaHC_5H_6O_4{\cdot}2H_2O)_n$ primary phase region			
0.2500	207.1		266.4
0.2500	208.8		267.3
0.2750	209.1	266.4	283.1
0.3000	208.6	266.4	290.6
0.3000	207.1		290.7
0.3250	206.6	266.1	297.2
0.3500 [e]	207.4	266.1	301.8
0.3750	207.6	266.1	305.5

[a] Experimental pressure was not controlled beyond the typical range of atmospheric pressure, (99.2 ± 2.9) kPa (station pressure).
[b] Mass fraction uncertainty, U = 0.0002 (0.95 confidence level).
[c] Temperature uncertainty, U = 0.9 K (0.94 confidence level).
[d] Melting of ice was identified by infrared spectroscopy of thin films as described in the Materials and Methods section.
[e] A solution of this concentration was used for X-ray crystallography experiments to determine the identity of the solid that is present at room temperature.

soluble salt. However, we see from the figure that the solubility data nearly coincide with those for $NaHC_4H_4O_4{\cdot}3H_2O$ in the binary system over a short concentration range. Thus, the presence of ammonium and sulfate ions in solution may prevent the trihydrate from forming because of strong ion-water attractions, allowing the anhydrous $NaHC_4H_4O_4$ to precipitate from solution as the least soluble salt. As the concentration of $NaHC_4H_4O_4$ decreases in the 0.1000 w_{AS} series, we note that the 0.1000 and 0.2000 w_{AS} data series become coincident at approximately 0.25 w $NaHC_4H_4O_4$ (0.85 NH_4^+/Na^+ mole ratio for 0.1000 w_{AS} and 1.7 NH_4^+/Na^+ mole ratio for 0.2000 w_{AS}). Lecontite was determined to be the least soluble salt for a 0.2000 w_{AS} sample (1.4 NH_4^+/Na^+ mole ratio). In a constant $(NH_4)_2SO_4$ data series the NH_4^+/Na^+ mole ratio increases as the concentration of $NaHC_4H_4O_4$ decreases. Thus, the formation of $NaNH_4SO_4{\cdot}2H_2O$ and subsequently $(NH_4)_2SO_4$ become more favorable from equilibrium considerations as the NH_4^+/Na^+ mole ratio increases:

$$NaHC_4H_4O_4(s) \rightleftharpoons Na^+(aq) + HC_4H_4O_4^-(aq) \quad (2)$$

$$NaNH_4SO_4 \cdot 2H_2O(s) \rightleftharpoons Na^+ + NH_4^+(aq) + SO_4^{2-}(aq) + 2H_2O(l) \quad (3)$$

$$(NH_4)_2SO_4(s) \rightleftharpoons 2NH_4^+(aq) + SO_4^{2-}(aq) \quad (4)$$

As seen in Eqs. (2)–(4), increasing ammonium ion concentration favours the left hand side of Eqs. (3) and (4). We believe this is what is observed in our 0.1000 w_{AS} data series. $NaHC_4H_4O_4$ is the least soluble salt at low NH_4^+/Na^+ mole ratios (0.61–0.85); however, as the ratio approaches unity, lecontite becomes less soluble. This interpretation is in agreement with the observation that the solubility data of 0.1000 and 0.2000 w_{AS} series become coincident at approximately unity NH_4^+/Na^+ mole ratio. We were not able to analyse crystals with solubilities below room temperature to confirm this conclusion because the temperature needed to maintain the precipitate is too low for transportation to the crystallographic facility we utilize.

The least soluble solid in a 0.3000 w_{AS} solution (2.5 NH_4^+/Na^+ mole ratio) is also lecontite, and its solubility is much lower than in the 0.2000 w_{AS} solutions. We do note a discontinuous change in slope of the solubility data for the 0.3000 w_{AS} solutions at 0.15 w $NaHC_4H_4O_4$ (NH_4^+/Na^+ mole ratio $\geq$4.2). This may be due to a change of the identity of the least soluble salt to ammonium sulfate as the NH_4^+/Na^+ ratio increases. Finally, for a 0.4000 w_{AS} solution (8.5 NH_4^+/Na^+ mole ratio), ammonium sulfate is the least soluble salt, and it is seen to be much less soluble than the other possible compounds at this concentration. Thus in general we find that increasing $(NH_4)_2SO_4$ in $NaHC_4H_4O_4$ solutions has a "salting out" effect, with the identity of the salt precipitated dependent on the NH_4^+/Na^+ mole ratio.

3.2.2. $Na_2C_4H_4O_4/(NH_4)_2SO_4/H_2O$

Raw DSC data for this system is given in TableS6 in the Supplementary material and shown in Fig. 3. From these results

Table 3
Identity of the least soluble solid in each ternary solution as determined by X-ray crystallographic analysis, w_{AS} = mass fraction $(NH_4)_2SO_4$, and w_{OS} = mass fraction of the organic salt as indicated, at pressure 99.2 kPa. [a]

w_{AS} [b]	Organic Salt	w_{OS}	Mole ratio NH_4^+/ Na^+	Least soluble solid
0.1000	$NaHC_4H_4O_4$	0.3500[c]	0.61	$NaHC_4H_4O_4$
0.2000	$NaHC_4H_4O_4$	0.3000[c]	1.4	$NaNH_4SO_4{\cdot}2H_2O$
0.3000	$NaHC_4H_4O_4$	0.2500[c]	2.5	$NaNH_4SO_4{\cdot}2H_2O$
0.4000	$NaHC_4H_4O_4$	0.1000[c]	8.5	$(NH_4)_2SO_4$
0.1000	$Na_2C_4H_4O_4$	0.3000[b]	0.41	$Na_2C_4H_4O_4{\cdot}6H_2O$
0.2000	$Na_2C_4H_4O_4$	0.2250[b]	1.1	$NaNH_4SO_4{\cdot}2H_2O$
0.3000	$Na_2C_4H_4O_4$	0.1501[b]	2.5	$NaNH_4SO_4{\cdot}2H_2O$
0.4000	$Na_2C_4H_4O_4$	0.1000[b]	4.9	$NaNH_4SO_4{\cdot}2H_2O$
0.1000	$NaHC_5H_6O_4$	0.3500[d]	0.67	$NaHC_5H_6O_4{\cdot}2H_2O$
0.2000	$NaHC_5H_6O_4$	0.3000[d]	1.6	$NaNH_4SO_4{\cdot}2H_2O$
0.3000	$NaHC_5H_6O_4$	0.2000[d]	3.5	$NH_4HC_5H_6O_4$
0.4000	$NaHC_5H_6O_4$	0.0900[d]	10.4	$NH_4HC_5H_6O_4$
0.1000	$Na_2C_5H_6O_4$	0.2500[b]	0.53	Na_2SO_4
0.2000	$Na_2C_5H_6O_4$	0.2000[b]	1.3	$NaNH_4SO_4{\cdot}2H_2O$
0.3000	$Na_2C_5H_6O_4$	0.1500[b]	2.7	$NaNH_4SO_4{\cdot}2H_2O$
0.4000	$Na_2C_5H_6O_4$	0.0700[b]	7.6	$NaNH_4SO_4{\cdot}2H_2O$

[a] Experimental pressure was not controlled beyond the typical range of atmospheric pressure, (99.2 ± 2.9) kPa (station pressure).
[b] Mass fraction uncertainty, U = 0.0001 (0.95 confidence level).
[c] Mass fraction uncertainty, U = 0.0008 (0.95 confidence level).
[d] Mass fraction uncertainty, U = 0.0002 (0.95 confidence level).

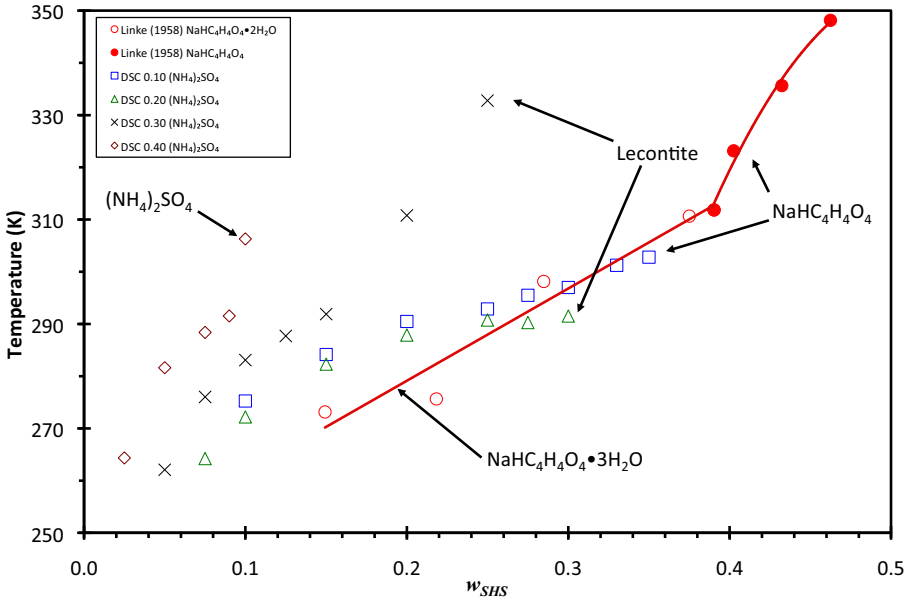

Fig. 2. Solubilities of salts for solutions of $NaHC_4H_4O_4/(NH_4)_2SO_4$ in water at mass fractions of ammonium sulphate as given in the legend, w_{SHS} is the mass fraction of $NaHC_4H_4O_4$. Identity of the least soluble solid from X-ray diffraction data at the concentrations given are indicated by arrows. Lines and curves are drawn to delineate phase boundaries in the binary organic salt/water system.

we conclude that for NH_4^+/Na^+ mole ratio $\leq$0.41 the least soluble solid is $Na_2C_4H_4O_4{\cdot}6H_2O$, which is the salt that precipitates from saturated $Na_2C_4H_4O_4/H_2O$ binary solutions at temperatures below 319 K. However, for higher concentrations of $(NH_4)_2SO_4$, NH_4^+/Na^+ mole ratio $\geq$ 1.09, the least soluble solid is $NaNH_4SO_4{\cdot}2H_2O$ (lecontite). Referring to Fig. 3, for 0.1000 w_{AS} solutions at high sodium succinate concentrations, we observe the salt solubility follows that of the binary solubility of $Na_2C_4H_4O_4{\cdot}6H_2O$ in water. However, a significant change in solubility is observed for solutions with $[Na_2C_4H_4O_4] \leq 0.2000$ *w*. One of two conclusions could be drawn from this observation. Either $(NH_4)_2SO_4$ begins to have a "salting out" effect on $Na_2C_4H_4O_4{\cdot}6H_2O$ at low $Na_2C_4H_4O_4$ concentrations, or at low $Na_2C_4H_4O_4$ concentrations a compound other than $Na_2C_4H_4O_4{\cdot}6H_2O$ is precipitating from solution. The 0.2000 w_{AS} data may provide some clue. Here we observe the least soluble solid for a 0.2250 *w* $Na_2C_4H_4O_4$ sample is lecontite. At lower $Na_2C_4H_4O_4$ concentrations (increasing NH_4^+/Na^+ mole ratio) the solubility data are coincident with that of the 0.1000 w_{AS} series. An interpretation of these results that would be consistent for both 0.1000 and 0.2000 w_{AS} data series would be that as the NH_4^+/Na^+ mole ratio increases in the 0.1000 w_{AS} series, the least soluble salt changes from $Na_2C_4H_4O_4{\cdot}6H_2O$ to lecontite at a NH_4^+/Na^+ mole ratio of approximately 1. Thus, the salt solubility in the two data series are coincident at this and higher NH_4^+/Na^+ mole ratios. Lecontite is again the least soluble salt in both the 0.3000 and 0.4000 w_{AS} series. However, here we note the solubility of lecontite is much less soluble than in the 0.2000 w_{AS} series. This is as expected since lecontite and ammonium sulfate have common ions (see Eq. (2)).

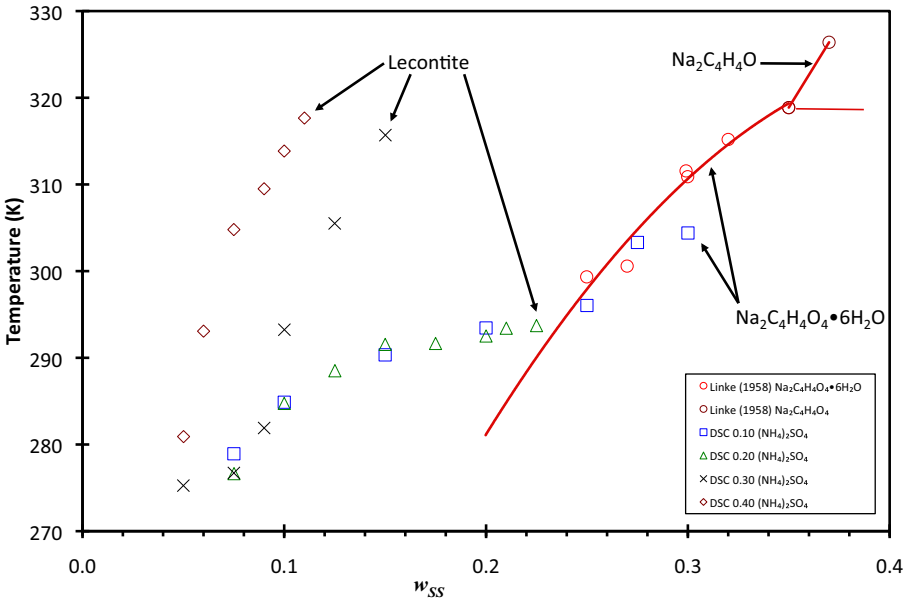

Fig. 3. Solubilities of salts for solutions of $Na_2C_4H_4O_4/(NH_4)_2SO_4$ in water at mass fractions of ammonium sulphate as given in the legend, w_{SS} is the mass fraction of $Na_2C_4H_4O_4$. Identity of the least soluble solid from X-ray diffraction data at the concentrations given are indicated by arrows. Lines and curves are drawn to delineate phase boundaries in the binary organic salt/water system.

3.2.3. $NaHC_5H_6O_4/(NH_4)_2SO_4/H_2O$

Raw DSC data for this system is given in Table S7 in the Supplementary material and shown in Fig. 4. From these results we conclude that for NH_4^+/Na^+ mole ratio $\leq$0.67 the least soluble solid is $NaHC_5H_6O_4{\cdot}2H_2O$, which is the salt that precipitates in the $NaHC_5H_6O_4/H_2O$ binary system. When the concentration of $(NH_4)_2SO_4$ is increased to 0.2000 w_{AS} with a NH_4^+/Na^+ mole ratio of 1.6, the least soluble solid is $NaNH_4SO_4{\cdot}2H_2O$ (lecontite). At higher concentrations as seen in the 0.3000 and 0.4000 w_{AS} series, the least soluble salt was found to be $NH_4HC_5H_6O_4$ (at 3.5 and 10 NH_4^+/Na^+ mole ratios). As seen in Fig. 4., for 0.1000 w_{AS} solutions at high sodium hydrogen glutarate concentrations (low NH_4^+/Na^+ mole ratios) the solubility data are close to the solubility of $NaHC_5H_6O_4{\cdot}2H_2O$ in the binary system, thus showing no effect from the presence of $(NH_4)_2SO_4$ on the solubility of this salt. However, as the NH_4^+/Na^+ mole ratio increases along the 0.1000 w_{AS} data series, the solubility clearly decreases as compared to the $NaHC_5H_6O_4/H_2O$ binary data, and in fact becomes essentially coincident with the 0.2000 w_{AS} data at 0.2000 w $NaHC_5H_6O_4$. At this point in the 0.1000 w_{AS} series, the NH_4^+/Na^+ mole ratio equals 1.2 and continues to increase as the concentration of $NaHC_5H_6O_4$ decreases. At this point in the 0.2000 w_{AS} series, the NH_4^+/Na^+ mole

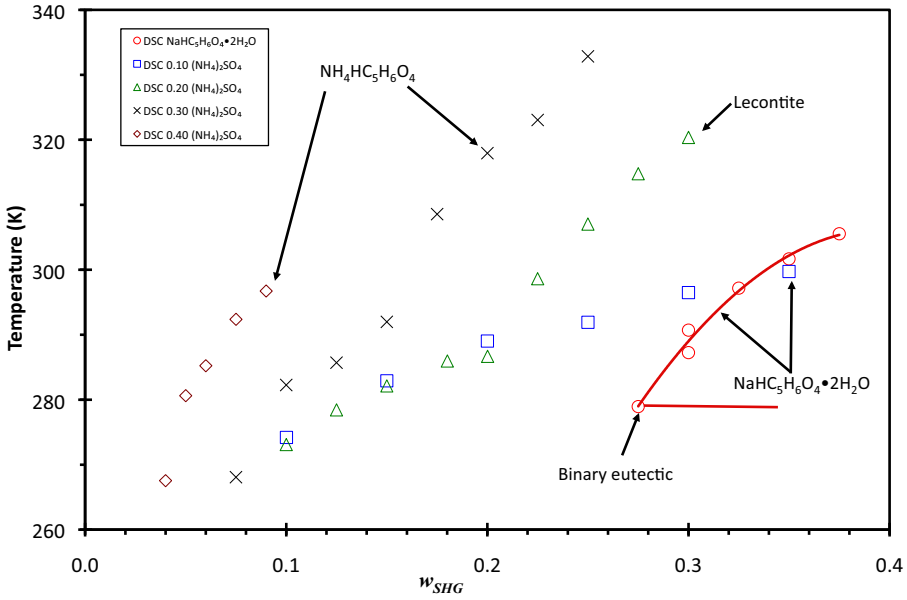

Fig. 4. Solubilities of salts for solutions of $NaHC_5H_6O_4/(NH_4)_2SO_4$ in water at mass fractions of ammonium sulphate as given in the legend, w_{SHG} is the mass fraction of $NaHC_5H_6O_4$. Identity of the least soluble solid from X-ray diffraction data at the concentrations given are indicated by arrows. Lines and curves are drawn to delineate phase boundaries in the binary organic salt/water system.

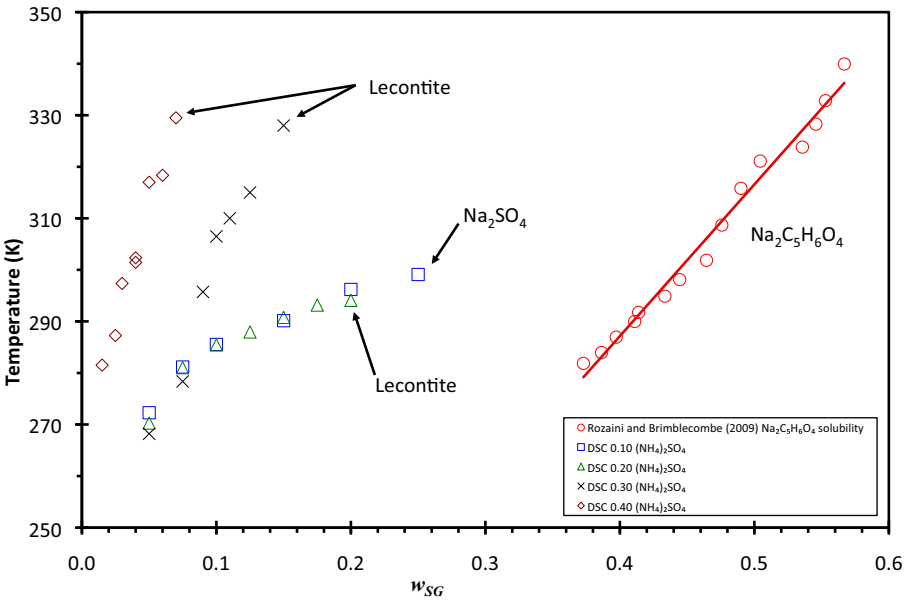

Fig. 5. Solubilities of salts for solutions of $Na_2C_5H_6O_4/(NH_4)_2SO_4$ in water at the concentrations given, w_{SG} is the mass fraction of $Na_2C_5H_6O_4$. Identity of the least soluble solid from X-ray diffraction data at the concentrations given are indicated by arrows. Red line delineates the binary phase boundary.

ratio is 2.3. Since lecontite was found to be the least soluble solid at a NH_4^+/Na^+ mole ratio of 1.6 (see Fig. 4), is seems likely that the least soluble solid in the 0.1000 w_{AS} series changes from $NaHC_5H_6O_4{\cdot}2H_2O$ to lecontite at a NH_4^+/Na^+ mole ratio of approximately 1. For the 0.3000 and 0.4000 w_{AS} series (3.5 and 10.4 NH_4^+/Na^+ mole ratio, respectively) the least soluble solid was determined to be $NH_4HC_5H_6O_4$, and this salt becomes less soluble with increasing $(NH_4)_2SO_4$ concentration, which is expected since NH_4^+ is a common ion:

$$NH_4HC_5H_6O_4(s) \rightleftharpoons NH_4^+(aq) + HC_5H_6O_4^-(aq) \quad (5)$$

3.2.4. $Na_2C_5H_6O_4/(NH_4)_2SO_4/H_2O$

Raw DSC data for this system is given in Table S8 in the Supplementary material and shown in Fig 5. From these results we conclude that for NH_4^+/Na^+ mole ratio $\leq$0.53 the least soluble solid is Na_2SO_4. However, for higher concentrations of $(NH_4)_2SO_4$, NH_4^+/Na^+ mole ratio $\geq$1.3, the least soluble solid is $NaNH_4SO_4{\cdot}2H_2O$ (lecontite). This is very similar to the $(NH_4)_2SO_4/Na_2C_4H_4O_4$ system where lecontite was the least soluble solid at 0.2000, 0.3000, and 0.4000 w_{AS}. However, we note that $Na_2C_5H_6O_4$ does not form even at 0.1000 w_{AS}, which indicates it remains very soluble even in the presence of additional ions in solution. This is not surprising; since it is the most soluble of the four organic salts we studied. Referring to Fig. 5, for 0.1000 w_{AS} solutions at high sodium succinate concentrations sodium sulfate is the least soluble solid; however, as the NH_4^+/Na^+ mole ratio decreases in that series, the solubilities of the 0.1000 and 0.2000 w_{AS} series coincide. It seems likely the least soluble solid in the 0.1000 w_{AS} series quickly becomes lecontite as the NH_4^+/Na^+ mole ratio drops (likely around a NH_4^+/Na^+ mole ratio equal to one). As ammonium sulfate concentrations increase (and NH_4^+/Na^+ mole ratios) lecontite becomes correspondingly less soluble. However, since NH_4^+ is a common ion between ammonium sulfate and lecontite, less Na^+ ions will remain in solution (from $NaC_5H_6O_4$) and thus the solubility of lecontite appears to decrease.

4. Discussion and atmospheric implications

The solubilities of the sodium salts of oxalic and malonic acid have previously been studied in our lab [24,25]. In both of those cases, we determined the order of solubility to be $H_2A > Na_2A > NaHA$, where A represents the organic anion. In this work we find glutaric acid and its sodium salts follow the same pattern, whereas succinic acid and its sodium salts follow the reverse ordering. We have compared the data sets in Fig. 6 where we plot the various solubilities. As an example, if we consider a temperature of 293 K, we observe that the order of solubility is $H_2C_3H_2O_4 > Na_2C_3H_2O_4 > H_2C_5H_6O_4 > NaHC_3H_2O_4{\cdot}H_2O > Na_2C_5H_6O_4 > NaHC_5H_6O_4{\cdot}2H_2O > NaHC_4H_4O_4{\cdot}3H_2O > Na_2C_4H_4O_4{\cdot}6H_2O > H_2C_2O_4{\cdot}2H_2O > H_2C_4H_4O_4 > Na_2C_2O_4 > NaHC_2O_4$. Thus when a range of dicarboxylic acids is present in atmospheric aerosols, with sodium ions, it is clear the sodium oxalates are the least soluble and will precipitate first. However, considering succinic acid, which is the least soluble of the four dicarboxylic acids we have studied, we observe that succinic acid will precipitate from solution before either of its sodium salts. Thus, partially or fully dissociated succinic acid in aerosols will be more soluble as sodium or disodium succinate. However, the impact on glutaric and malonic acid will be the opposite (but the same as oxalic acid) in the presence of sodium ions. Clearly sodium salt solubility does not follow the "even-odd" pattern of solubility of the dicarboxylic acids where even numbered carbon acids are less soluble than odd numbered ones [38,39]. In fact, there is overlap in the solubilities of $NaHC_4H_4O_4{\cdot}3H_2O$ and $NaHC_5H_6O_4{\cdot}2H_2O$, even though their acid solubilities are very different. Saxena and Hildemann [40] expected dicarboxylic acids in atmospheric aerosols that were neutralized by strong alkaline ions such as Na^+ and K^+ would be more soluble than their parent acids. However, they based this expectation on the solubility of the sodium succinate salts, which we now know is the exception rather than the rule. Thus, the explanation for a broader pattern of sodium salt solubility of the dicarboxylic acids remains uncertain.

Introducing ammonium and sulfate ions significantly alters the physical chemistry of these aqueous systems. At minimum the formation of additional solids is now possible: $(NH_4)_2SO_4$, Na_2SO_4 ($Na_2SO_4{\cdot}10H_2O$), and $NaNH_4SO_4{\cdot}2H_2O$ (lecontite). Additionally, the presence of ammonium and sulfate may have a salting in or salting out effect on compounds that can form. We have plotted the solubility of ammonium sulfate [35], sodium sulfate, sodium sulfate decahydrate [22], succinic acid [38], and its sodium salts

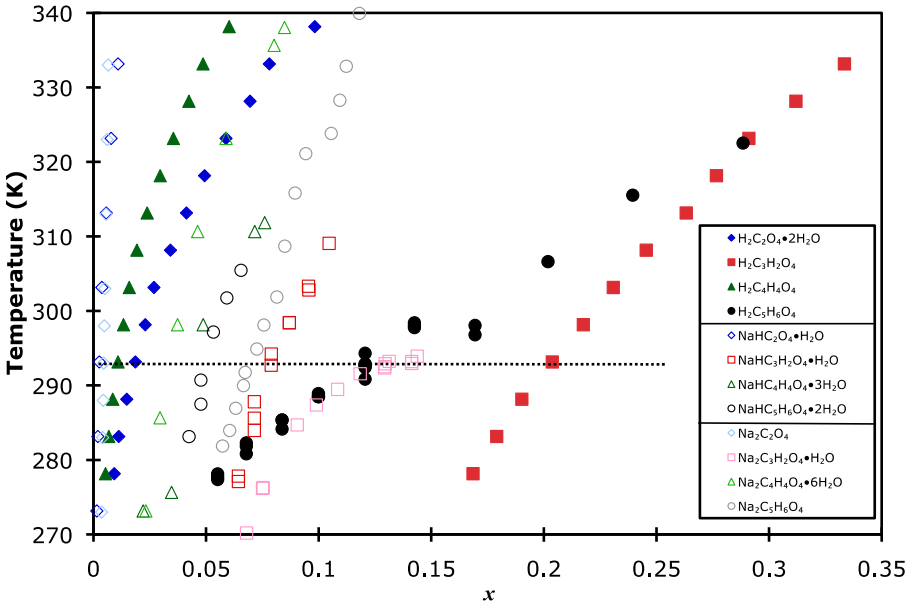

Fig. 6. Solubilities of oxalic acid dihydrate [38], malonic acid [41], succinic acid [38], glutaric acid [41], sodium hydrogen oxalate monohydrate [22], sodium hydrogen malonate monohydrate [24], sodium hydrogen succinate trihidrate [22], sodium hydrogen glutarate (this work), sodium oxalate [35], sodium malonate monohydrate [24], sodium succinate hexahydrate [22], and sodium glutarate [23] as a function of temperature, x represents the mole fraction of each solute. Dotted line is at T = 293 K. The legend is divided into three groups from top to bottom: organic acids, monosodium organic salts, disodium organic salts. Compounds with the same root organic anion have the same symbol shape and same color group in the figure.

[22] in Fig. 7. In terms of water solubility, $(NH_4)_2SO_4$ is significantly more soluble than succinic acid or its sodium salts while the solubility of sodium sulfate and its decahydrate salt lie between that of succinic acid and its sodium salts. Referring to Figs. 2 and 3, we observe that a low concentration of ammonium sulfate has little impact on the solubility of $NaHC_4H_4O_4$ or $Na_2C_4H_4O_4{\cdot}6H_2O$. However, in both cases, moderate amounts of ammonium sulfate cause $NaNH_4SO_4{\cdot}2H_2O$ (lecontite) to be the least soluble solid. Thus it would appear that the solubility of lecontite must either lie somewhere to the left of the solubility data of the sodium salts of succinic acid in Fig. 7, or ammonium sulfate has a salting in effect on these salts such that they become more soluble than lecontite, which in turn must be less soluble than ammonium sulfate. This seems to be the case for all concentrations of $Na_2C_4H_4O_4$ we studied, since lecontite was found to be the least soluble solid at moderate to high ammonium sulfate concentrations. However, ammonium sulfate becomes the least soluble solid in the presence of $NaHC_4H_4O_4$ (Fig. 2) at high $(NH_4)_2SO_4$ concentration, which supports the theory that ammonium sulfate is having a salting in effect on the sodium salts of succinic acid. These observations are not what would be expected from the binary aqueous solubility data alone as shown in Fig. 7. Here we see that at high sodium and sulfate ion concentrations, the least soluble salts over a wide temperature range are Na_2SO_4 at T > 305 K, and $Na_2SO_4{\cdot}10H_2O$ at T $\leq$ 305 K. However, we did not observe the formation of sodium sulfate or its hydrate in any of our ammonium sulfate/sodium or sodium hydrogen succinate samples. What we did observe in solutions with both 1:1 and 2:1 Na:succinate ratios in the presence of ammonium sulfate is the mineral lecontite ($NaNH_4SO_4{\cdot}2H_2O$). This is similar to what we observed in our study of the effect of ammonium sulfate on solutions of the sodium salts of malonic acid [24], where we discussed in greater detail the conditions under which lecontite can form. Lecontite has no actual solubility equilibrium in aqueous solution without other species present and thus can not be represented on Figure 7. High concentrations of ammonium ions and moderate to high concentrations of sodium and sulfate ions are necessary for lecontite to form from aqueous solution as shown by the $Na_2SO_4/(NH_4)_2SO_4/H_2O$ solubility data (Fig. S1 in Supporting Information of Kissinger et al. [24]). Thus at moderate to low ammonium concentrations in atmospheric aerosols in the presence of sodium, sulfate, and hydrogen succinate or succinate ions we would expect the formation of one of the sodium succinate salts as droplets evaporate or cool. However, as ammonium and sulfate ion concentrations increase, it is possible to move into a concentration region where lecontite is the least soluble substance, an observation that would not be predicted from theory alone.

A similar comparison of solubilities for glutaric acid [41], $NaHC_5H_6O_4{\cdot}2H_2O$, and $Na_2C_5H_6O_4$ [23] is given in Fig. 8 as a function of mole fraction of solute. We see glutaric acid is more soluble than its sodium salts, with the least soluble being $NaHC_5H_6O_4{\cdot}2H_2O$. However, the solubility of glutaric acid intersects that of sodium glutarate at approximately 278 K. The affect of ammonium and sulfate ions in the glutarate system depends on whether a 1:1 or 2:1 ratio of Na^+:$H_2C_5H_6O_4$ is present in solution. Referring to Fig. 4, we observe that at the lowest concentration of ammonium sulfate there is little effect on the $NaHC_5H_6O_4{\cdot}2H_2O$ solubility at the lowest NH_4^+:Na^+ ratio; however, as the ratio increases we observe an increasing salting out effect on $NaHC_5H_6O_4{\cdot}2H_2O$ until the point is reached at a ratio of approximately 1 to 2 where we believe lecontite becomes the least soluble solid as discussed in the Results section. At moderate concentrations of ammonium sulfate (higher NH_4^+:Na^+ ratios) lecontite was found to be the least soluble solid. Thus, lecontite solubility must lie to the left of that for sodium sulfate in Fig. 8. At high ammonium sulfate concentrations ammonium hydrogen glutarate is the least soluble solid. Solubilities for this salt have not been measured to our knowledge, so we are unable to conclude whether ammonium sulfate is having an effect on its solubility in this mixed system; however, high ammonium concentrations clearly make this salt less soluble than lecontite and sodium sulfate.

Finally, if we consider the effect of ammonium sulfate on solutions that are 2:1 Na^+:$H_2C_5H_6O_4$, we observe a different effect. As seen in Fig. 5, at low ammonium sulfate concentrations the least soluble solid is sodium sulfate. This observation may not be

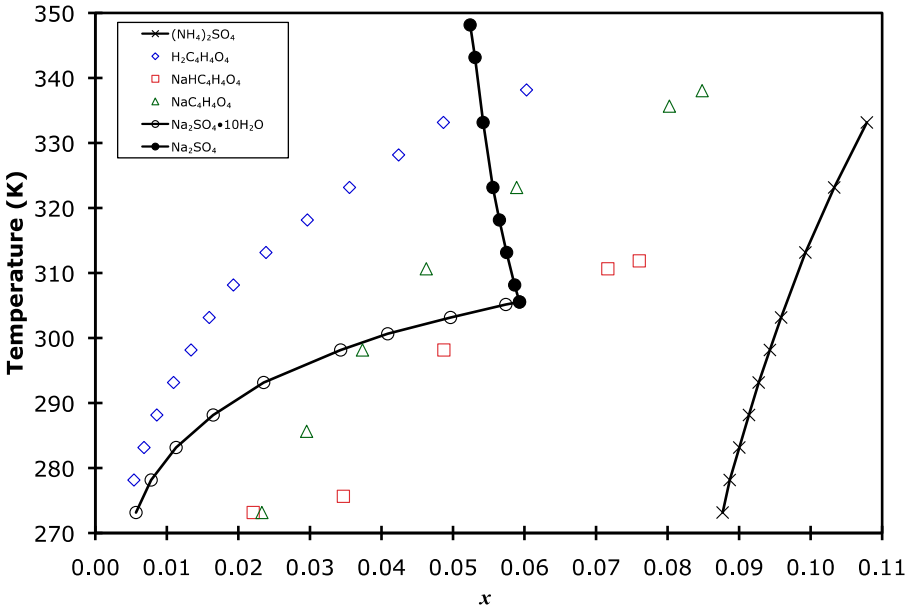

Fig. 7. Solubilities of succinic acid [38], sodium hydrogen succinate trihidrate [22], sodium succinate hexahydrate [22], ammonium sulfate [35], sodium sulfate, and sodium sulfate decahydrate [22] as a function of temperature. Curves are drawn to connect the solubility points of the inorganic salts for clarity, and *x* represents the mole fraction of each solute.

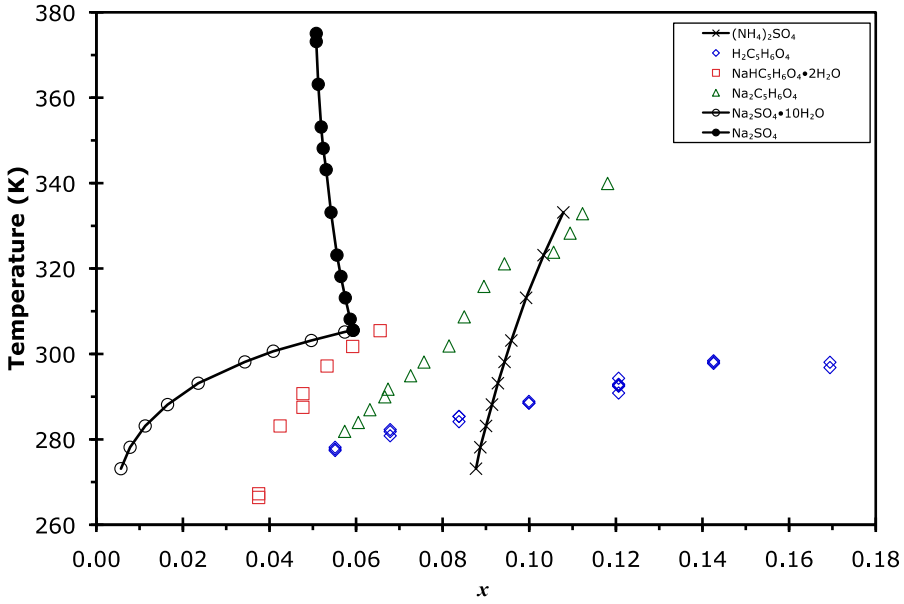

Fig. 8. Solubilities of glutaric acid [41], sodium hydrogen glutarate dihidrate (this work), sodium glutarate [23], ammonium sulfate [35], sodium sulfate and sodium sulfate decahydrate [22] as a function of temperature. Curves are drawn to connect the solubility points of the inorganic salts for clarity.

surprising since sodium sulfate has the lowest water solubility among the other salts present (Fig. 8). However, when the ammonium sulfate concentration is increased, lecontite becomes the least soluble solid, and this remains the case for the moderate to high ammonium sulfate concentrations we studied. In fact, even at low ammonium sulfate concentrations, it appears lecontite is the least soluble solid as NH_4^+:Na^+ ratios approach or exceed unity, as discussed in the Results section. Thus, in this scenario, we find again lecontite is dominates as the least soluble solid over a wide concentration and temperature range.

Our conclusion from these data is that regardless of the specific dicarboxylic acid, when ammonium, sodium and sulfate ions are present in aqueous solution, lecontite is most often the least soluble solid. It was found to be the least soluble solid in at least 56% of the concentration series we studied (9 of 16), and was likely present in more samples when NH_4^+:Na^+ ratio increased past unity. Thus, this is clearly a salt that needs further study with respect to its solubility in other chemical systems, and its impact on aerosol chemistry and other physical processes.

5. Conclusions

We have studied the solubility of the sodium salts of succinic and glutaric acids with and without ammonium sulfate present. As we have observed in other systems, we determined that the least soluble solids are most often not the organic sodium salts or ammonium sulfate, but rather a salt made up of the ions present, namely lecontite. This is a mineral that has been generally overlooked in the literature in terms of its presence in atmospheric aerosols. However, we have determined in this study, that it is often the least soluble salt under varying concentration conditions (56% of samples studied). In 19% of samples the organic salt was the least soluble compound and in 6% it was $(NH_4)_2SO_4$. For the system involving 1:1 Na^+:$H_2C_5H_6O_4$ and ammonium sulfate, at high ammonium concentrations $NH_4HC_5H_6O_4$ was the least soluble salt (12% of samples studied). Thus, it becomes clear that salts made up of various combinations of the ions present in atmospheric aerosols must be considered when predicting compounds that may form in these aerosols. We have also determined for the first time the solubility and ice melting temperatures in the $NaHC_5H_6O_4/H_2O$ system.

Acknowledgements

We wish to thank Anastasiya Vinokur and Dr. Ilia Guzei at the University of Wisconsin-Madison for running and analyzing the X-ray crystallography experiments.

Funding

This work was supported by the National Science Foundation (USA) Atmospheric Chemistry Program (AGS-1361592)

Declaration of interests

None.

Appendix A. Supplementary data

Supplementary data associated with this article can be found, in the online version, at https://doi.org/10.1016/j.jct.2018.06.002.

References

[1] D.M. Murphy, D.S. Thomson, T.M.J. Mahoney, In situ measurements of organics, meteoritic material, mercury, and other elements in aerosols at 5 to 19 kilometers, Science 282 (1998) 1664–1669.
[2] K.D. Froyd, D.M. Murphy, P. Lawson, D. Baumgardner, R.L. Herman, Aerosols that form subvisible cirrus at the tropical tropopause, Atmos. Chem. Phys. 10 (2010) 209–218, https://doi.org/10.5194/acp-10-209-2010.
[3] J.H. Seinfeld, S.N. Pandis, Atmospheric Chemistry and Physics: From Air Pollution to Climate Change, Wiley, New York, 1998.
[4] R.C. Sullivan, K.A. Prather, Investigations of the diurnal cycle and mixing state of oxalic acid in individual particles in Asian aerosol outflow, Environ. Sci. Technol. 41 (2007) 8062–8069, https://doi.org/10.1021/es071134g.
[5] S. Kundu, K. Kawamura, M. Kobayashi, E. Tachibana, M. Lee, P.Q. Fu, J. Jung, A sub-decadal trend in diacids in atmospheric aerosols in eastern Asia, Atmos. Chem. Phys. 16 (2016) 585–596, https://doi.org/10.5194/acp-16-585-2016.
[6] M. Hallquist, J.C. Wenger, U. Baltensperger, Y. Rudich, D. Simpson, M. Claeys, J. Dommen, N.M. Donahue, C. George, A.H. Goldstein, J.F. Hamilton, H. Herrmann, T. Hoffmann, Y. Iinuma, M. Jang, M.E. Jenkin, J.L. Jimenez, A. Kiendler-Scharr, W. Maenhaut, G. McFiggans, T.F. Mentel, A. Monod, A.S.H. Prévôt, J.H. Seinfeld, J.D. Surratt, R. Szmigielski, J. Wildt, The formation, properties and impact of secondary organic aerosol: current and emerging issues, Atmos. Chem. Phys. 9 (2009) 5155–5236, https://doi.org/10.5194/acp-9-5155-2009.
[7] D.K. Deshmukh, K. Kawamura, M. Lazaar, B. Kunwar, S.K.R. Boreddy, Dicarboxylic acids, oxoacids, benzoic acid, α-dicarbonyls, WSOC, OC, and ions in spring aerosols from Okinawa Island in the western North Pacific Rim: size distributions and formation processes, Atmos. Chem. Phys. 16 (2016) 5263–5282, https://doi.org/10.5194/acp-16-5263-2016.
[8] E. Harris, B. Sinha, S. Foley, J.N. Crowley, S. Borrmann, P. Hoppe, Sulfur isotope fractionation during heterogeneous oxidation of SO_2 on mineral dust, Atmos. Chem. Phys. 12 (2012) 4867–4884, https://doi.org/10.5194/acp-12-4867-2012.
[9] P. Reitz, C. Spindler, T.F. Mentel, L. Poulain, H. Wex, K. Mildenberger, D. Niedermeier, S. Hartmann, T. Clauss, F. Stratmann, R.C. Sullivan, P.J. DeMott, M. D. Petters, B. Sierau, J. Schneider, Surface modification of mineral dust particles by sulphuric acid processing: implications for ice nucleation abilities, Atmos. Chem. Phys. 11 (2011) 7839–7858, https://doi.org/10.5194/acp-11-7839-2011.
[10] E. Harris, B. Sinha, D. van Pinxteren, A. Tilgner, K.W. Fomba, J. Schneider, A. Roth, T. Gnauk, B. Fahlbusch, S. Mertes, T. Lee, J. Collett, S. Foley, S. Borrmann, P. Hoppe, H. Herrmann, Enhanced role of transition metal ion catalysis during in-cloud oxidation of SO_2, Science 340 (2013) 727–730, https://doi.org/10.1126/science.1230911.
[11] V.-M. Kerminen, K. Teinilä, R. Hillamo, T. Pakkanen, Substitution of chloride in sea-salt particles by inorganic and organic anions, J. Aerosol. Sci. 29 (1998) 929–942, https://doi.org/10.1016/S0021-8502(98)00002-0.
[12] T. Kojima, P.R. Buseck, Y. Iwasaka, A. Matsuki, D. Trochkine, Sulfate-coated dust particles in the free troposphere over Japan, Atmos. Res. 82 (2006) 698–708, https://doi.org/10.1016/j.atmosres.2006.02.024.
[13] A. Laskin, R.C. Moffet, M.K. Gilles, J.D. Fast, R.A. Zaveri, B. Wang, P. Nigge, J. Shutthanandan, Tropospheric chemistry of internally mixed sea salt and organic particles: Surprising reactivity of NaCl with weak organic acids, J. Geophys. Res. 117 (2012) D15302, https://doi.org/10.1029/2012JD017743.
[14] J.S. Reid, R. Koppmann, T.F. Eck, D.P. Eleuterio, A review of biomass burning emissions part II: intensive physical properties of biomass burning particles, Atmos. Chem. Phys. 5 (2005) 799–825, https://doi.org/10.5194/acp-5-799-2005.
[15] M.D. Zauscher, Y. Wang, M.J.K. Moore, C.J. Gaston, K.A. Prather, Air quality impact physicochemical aging of biomass burning aerosols during the, San Diego Wildfires, Environ. Sci. Technol. 47 (2013) (2007) 7633–7643, https://doi.org/10.1021/es4004137.
[16] K.-P. Hinz, A. Trimborn, E. Weingartner, S. Henning, U. Baltensperger, B. Spengler, Aerosol single particle composition at the Jungfraujoch, J. Aerosol Sci. 36 (2005) 123–145, https://doi.org/10.1016/j.jaerosci.2004.08.001.
[17] D.M. Murphy, D.J. Cziczo, K.D. Froyd, P.K. Hudson, B.M. Matthew, A.M. Middlebrook, R.E. Peltier, A. Sullivan, D.S. Thomson, R.J. Weber, Single-particle mass spectrometry of tropospheric aerosol particles, J. Geophys. Res. Atmos. 111 (2006), https://doi.org/10.1029/2006JD007340.
[18] R.C. Sullivan, S.A. Guazzotti, D.A. Sodeman, K.A. Prather, Direct observations of the atmospheric processing of Asian mineral dust, Atmos. Chem. Phys. 7 (2007) 1213–1236, https://doi.org/10.5194/acp-7-1213-2007.
[19] D.J. Cziczo, K.D. Froyd, C. Hoose, E.J. Jensen, M. Diao, M.A. Zondlo, J.B. Smith, C. H. Twohy, D.M. Murphy, Clarifying the dominant sources and mechanisms of cirrus cloud formation, Science 340 (2013) 1320–1324, https://doi.org/10.1126/science.1234145.
[20] S. Ghorai, B. Wang, A. Tivanski, A. Laskin, Hygroscopic properties of internally mixed particles composed of NaCl and water-soluble organic acids, Environ. Sci. Technol. 48 (2014) 2234–2241, https://doi.org/10.1021/es404727u.
[21] B. Wang, R.E. O'Brien, S.T. Kelly, J.E. Shilling, R.C. Moffet, M.K. Gilles, A. Laskin, Reactivity of liquid and semisolid secondary organic carbon with chloride and nitrate in atmospheric aerosols, J. Phys. Chem. A 119 (2015) 4498–4508, https://doi.org/10.1021/jp510336q.
[22] W.F. Linke, Solubilities: inorganic and metal organic compounds: A revision and continuation of the compilation by A. Seidell. Fourth Edition. TWO VOLUMES, 4th edition, Van Nostrand, 1958.
[23] M.Z.H. Rozaini, P. Brimblecombe, The solubility measurements of sodium dicarboxylate salts; sodium oxalate, malonate, succinate, glutarate, and adipate in water from T = (279.15 to 358.15) K, J. Chem. Thermodyn. 41 (2009) 980–983, https://doi.org/10.1016/j.jct.2009.03.017.
[24] J.A. Kissinger, L.G. Buttke, A.I. Vinokur, I.A. Guzei, K.D. Beyer, Solubilities and glass formation in aqueous solutions of the sodium salts of malonic acid with and without ammonium sulfate, J. Phys. Chem. A 120 (2016) 3827–3834, https://doi.org/10.1021/acs.jpca.6b02656.
[25] L.G. Buttke, J.R. Schueller, C.S. Pearson, K.D. Beyer, Solubility of the sodium and ammonium salts of oxalic acid in water with ammonium sulfate, J. Phys. Chem. A 120 (2016) 6424–6433, https://doi.org/10.1021/acs.jpca.6b05208.
[26] P.R. Mallinson, C.S. Frampton, Structure of sodium hydrogen succinate at 123 K, Acta Crystallogr. C 48 (1992) 1555–1556, https://doi.org/10.1107/S0108270192006310.
[27] I. Fonseca, S. Martínez-Carrera, S. García-Blanco, Structure of sodium succinate hexahydrate, Acta Crystallogr. C 42 (1986) 1123–1125, https://doi.org/10.1107/S0108270186093174.
[28] A.L. Macdonald, P. Morrison, A. Murray, A.A. Freer, Structure of sodium hydrogen glutarate dihydrate, Acta Crystallogr. C 47 (1991) 728–730, https://doi.org/10.1107/S0108270190010459.
[29] A.L. Macdonald, J.C. Speakman, Rubidium hydrogen glutarate and ammonium hydrogen glutarate: X-ray studies of quasi-isostructural crystals involving very short hydrogen bonds, J. Cryst. Mol. Struct. 1 (1971) 189–198, https://doi.org/10.1007/BF01198531.
[30] S. Arzt, A.M. Glazer, The optical activity and absolute optical chirality of $NaNH_4SO_4.2H_2O$, Acta Crystallogr. B 50 (1994) 425–431, https://doi.org/10.1107/S0108768193014569.
[31] V.V. Udalova, Z.G. Pinsker, Electron diffraction study of the structure of ammonium sulfate, Sov. Phys. Crystallogr. Transl. Krist. 8 (1964) 433–440.

[32] S.E. Rasmussen, J.E. Jørgensen, B. Lundtoft, Structures and phase transitions of Na_2SO_4, J. Appl. Crystallogr. 29 (1996) 42–47, https://doi.org/10.1107/S0021889895008818.
[33] M. Schubnell, Temperature and heat flow calibration of a DSC-instrument in the temperature range between-100 and 160 degrees C, J. Therm. Anal. Calorim. 61 (2000) 91–98.
[34] D.R. Lide, Handbook of Chemistry and Physics, CRC Press, Boca Ratan, 1993.
[35] H. Stephen, T. Stephen, H.L. Silcock, Solubilities of Inorganic and Organic Compounds, Pergamon Press; Macmillan, [Oxford] New York, 1963.
[36] H. Marshall, D. Bain, LXXXVIII.—Sodium succinates, J. Chem. Soc. Trans. 97 (1910) 1074–1085, https://doi.org/10.1039/CT9109701074.
[37] R. Taft, F.H. Welch, Physical properties of aqueous solutions of sodium oxalate, sodium malonate, and sodium succinate, I, Trans. Kans. Acad. Sci. 1903- 54 (1951) 233, https://doi.org/10.2307/3625790.
[38] A. Apelblat, E. Manzurola, Solubility of oxalic, malonic, succinic, adipic, maleic, malic, citric, and tartaric-acids in water from 278.15-K to 338.15-K, J. Chem. Thermodyn. 19 (1987) 317–320.
[39] A. Apelblat, E. Manzurola, Solubility of ascorbic, 2-furancarboxylic, glutaric, pimelic, salicylic, and o-phthalic acids in water from 279.15 to 342.15 K, and apparent molar volumes of ascorbic, glutaric, and pimelic acids in water at 298.15 K, J. Chem. Thermodyn. 1005–1008 (21 1989), https://doi.org/10.1016/0021-9614(89)90161-4.
[40] P. Saxena, L.M. Hildemann, Water-soluble organics in atmospheric particles: a critical review of the literature and application of thermodynamics to identify candidate compounds, J. Atmos. Chem. 24 (1996) 57–109, https://doi.org/10.1007/BF00053823.
[41] K.D. Beyer, K. Friesen, J.R. Bothe, B. Palet, Phase diagrams and water activities of aqueous dicarboxylic acid systems of atmospheric importance, J. Phys. Chem. A 112 (2008) 11704–11713.

JCT 2018-60